Published in final edited form as:
Proteins. 2012 October ; 80(10): 2469–2475. doi:10.1002/prot.24140.

The Catalytic Domain of the Germination-Specific Lytic Transglycosylase SleB from *Bacillus anthracis* Displays a Unique Active Site Topology

Xing Jing[1], **Howard R. Robinson**[2], **Jared D. Heffron**[3], **David L. Popham**[1], and **Florian D. Schubot**[1,*]

[1]Virginia Tech Department of Biological Sciences Life Sciences 1 - MC0910 Washington Street Blacksburg, VA 24061

[2]Biology Department, Brookhaven National Laboratory, Upton, NY 11973-5000

Abstract

Bacillus anthracis produces metabolically inactive spores. Germination of these spores requires germination-specific lytic enzymes (GSLEs) that degrade the unique cortex peptidoglycan to permit resumption of metabolic activity and outgrowth. We report the first crystal structure of the catalytic domain of a GSLE, SleB. The structure revealed a transglycosylase fold with unique active site topology and permitted identification of the catalytic glutamate residue. Moreover, the structure provided insights into the molecular basis for the specificity of the enzyme for muramic-δ-lactam-containing cortex peptidoglycan. The protein also contains a metal-binding site that is positioned directly at the entrance of the substrate-binding cleft.

Keywords

SleB; CwlJ; *Bacillus anthracis*; spore; germination; lytic transglycosylase; muramic-δ-lactam; peptidoglycan; cortex peptidoglycan

Introduction

Bacterial endospores can survive in a metabolically dormant state for many years and exhibit extreme resistance to a wide range of killing agents [1]. Dormancy and most resistance properties are dependent on the relative dehydration of the spore core (cytoplasm), and this dehydration is dependent on the presence of the spore cortex peptidoglycan (PG) wall surrounding the core [1]. When spores sense a favorable growth environment and initiate germination, they must degrade the cortex PG as an essential step to allow full core rehydration and a resumption of metabolism [2,3]. The germination-specific lytic enzymes (GSLEs) responsible for cortex degradation are produced during spore formation and are held in a highly stable yet inactive state during spore dormancy. The mechanism by which GSLEs are held inactive, their mechanism of activation, and the molecular basis for their specificity for the cortex PG are of basic as well as applied interest. Treatments that activate GSLEs result in a loss of spore resistance properties [4]. A method of triggering highly efficient and synchronous activation of GSLEs would therefore greatly simplify spore

[*]**Corresponding author** Contact Information: **Florian Schubot, Ph. D.** Assistant Professor Virginia Polytechnic Institute and State University Department of Biological Sciences Life Science 1, Room 125 Blacksburg, VA 24061 fschubot@vt.edu Phone: (540) 231-2393 Fax: 540.231.4043.
[3]**Current Address:** USAMRIID Bacteriology Division Frederick, MD 21702-5011

decontamination measures, which is relevant for clinical spaces, food preparation facilities, and anti-bioweapon development.

The GSLE SleB has been shown to play a key role in the germination of spores of several *Bacillus* species [5-7], and *sleB* genes are highly conserved across the *Bacillus* genus as well as in some *Clostridium* species [8]. SleB is produced within the developing spore with a signal peptide that is cleaved following SleB translocation across the spore membrane [7,9,10]. SleB then remains inactive within the same spore compartment as the cortex PG and is activated during germination. Active SleB functions as a lytic transglycosylase to depolymerize the cortex PG [5,6]. SleB and other GSLEs exhibit specificity for PG containing the modified sugar muramic-δ-lactam [2,11,12], which is found only within spore cortex PG [13].

In addition to its catalytic domain (pfam07486)[14] SleB possesses an N-terminal PG-binding domain (pfam01471)[7,10,15], which increases its affinity for PG and its rate of PG cleavage although it is not required for either role [15]. Interestingly, a second GSLE, CwlJ, possesses significant sequence similarity with the catalytic domain of SleB but lacks the PG-binding domain [14].

To begin characterization of SleB substrate recognition and cleavage factors, we have determined the crystal structure of the catalytic domain of *B. anthracis* SleB ($SleB_{CAT}$) to 1.9 Å resolution. While it shares some features with other transglycosylases, $SleB_{CAT}$ displays a unique binding cleft topology reflective of its unusual specificity for muramic-δ-lactam-containing PG. The structure also revealed the catalytic glutamate residue and led to the unexpected discovery of a metal binding site, which is conspicuously positioned at the entrance of the substrate-binding pocket.

Materials and Methods

Expression and purification of SleB and $SleB_{CAT}$

The expression vectors and protocols used for full-length SleB and $SleB_{CAT}$ were identical to those used in a previous study [15] with minor modifications. Protein expression was induced at 20°C rather than 10°C. Cells were resuspended in 5 ml buffer A (50 mM Tris-HCl, 150 mM NaCl, 25 mM imidazole, pH 7.4), 1mM DTT, and 0.3 mM phenylmethanesulfonyl fluoride (Sigma) per gram cells. Cell lysis via sonication was followed by centrifugation at 40,000 x*g* for 30 min. The supernatant was filtered through a 0.45 μm polyethersulfone membrane and loaded onto to a 30-mL Ni-NTA Superflow column (Qiagen) pre-equilibrated in buffer A. The column was washed with buffer A and eluted with a linear imidazole gradient to 250 mM. Cleavage of the HisMBP fusion proteins was achieved by adding a variant of Tobacco Etch Virus protease, His-TEV(S219V)-Arg (1.5 mg TEV per 10 mg of total protein) to the pooled peak fractions. The reaction mixture was dialyzed overnight into buffer A. Subsequently, the protein solution was filtered and applied to a 40-mL Ni-NTA Superflow column (Qiagen) pre-equilibrated with buffer A. Flow-through fractions containing the SleB or $SleB_{CAT}$ were dialyzed overnight into 50 mM Tris, 50 mM NaCl, pH 7.5 and 2 mM DTT with 2.5% glycerol (buffer B). The sample was then applied to a 10-mL Heparin column (GE Healthcare) pre-equilibrated with buffer B and was eluted with a linear gradient to 0.5 M NaCl. Peak fractions were concentrated and loaded onto a HiPrep 26/60 Superdex™200 prep grade column (GE Healthcare) pre-equilibrated in a buffer of 25 mM Tris-HCl, 150 mM NaCl, 2mM tris (2-carboxyethyl) phosphine and 2.5% glycerol, pH 7.4 (buffer C). The protein was judged to be >95% pure by sodium dodecyl sulfate-polyacrylamide gel electrophoresis.

Cloning, expression, and purification of selenomethionine-substituted $SleB_{CAT}$ and $SleB_{CAT}^{L143M}$

Because the single methionine in the native sequence of $SleB_{CAT}$ proved insufficient for structure solution a second methionine was introduced in position 143 via site-directed mutagenesis using the following primers: 5'-TGATATTCAGATGATGGCAAACGCAGTATATGGA-3' and 5'-CGTTTGCCATCATCTGAATATCATTTTGAGAATA-3'. After sequencing, the modified plasmid was transformed into *E. coli* BL21 (DE3) CodonPlus RIL cells (Stratagene, La Jolla, CA) for protein expression.

To prepare selenomethionine-substituted $SleB_{CAT}$ or $SleB_{CAT}^{L143M}$, cells obtained from a 1 L of mid-log phase culture (prepared as described above) were washed twice in 100 mL of M9 selenomethionine growth media (Medicilon). The cells were resuspended in 100 mL of M9 selenomethionine growth media and used to inoculate four 1 L cultures containing M9 selenomethionine growth media and antibiotics. These cultures were grown with agitation at 37°C until the OD_{600nm} reading reached 0.5. Protein expression and purification followed the same procedures as described above.

Crystallization of native $SleB_{CAT}$ and $SleB_{cat}^{L143M}$

Crystallization screening in the sitting-drop format produced an initial hit from condition F7 of the IndexHT screen (Hampton Research). Hit optimization was carried out using the hanging drop vapor diffusion method at room temperature (23°C). Diffraction quality crystals for both native $SleB_{CAT}$ and SeMet-$SleB_{CAT}^{L143M}$ were obtained from droplets containing a 1:1 mixture of 2.5 mg/mL protein and a crystallization solution composed of 0.2 M ammonium sulfate, 0.1 M Bis-Tris (pH 5.8) and 15% w/v polyethylene glycol 3350.

Data collection, structure solution, and refinement

Crystals were loop-mounted after they had been soaked in a cryo-solution consisting of crystallization stock solution supplemented with either 10% or 12.5% glycerol, and subsequently flash-frozen in liquid nitrogen. All data sets were collected at beamline X-29A of Brookhaven National Laboratory using an ADSC Q315 CCD detector. The CCP4 program suite [16] was used for data processing.

Multiple wavelength anomalous dispersion (MAD) data collection [17] of the $SleB_{CAT}^{L143M}$ variant crystal yielded excellent electron density maps used for model building. Selenium atom search, initial phase calculation, density modification, and automated model building were all completed in the PHENIX program suite [18]. Iterative cycles of manual model adjustment using COOT [19] followed by refinement in PHENIX converged to produce the final structures. Detailed statistics for data collection, experimental phasing, and model refinement are provided in Table I. The model quality was validated using Procheck [20]. The coordinates for the two molecules in the asymmetric unit have been deposited with the Protein Data Bank (pdb code 4FET).

Construction of active site mutant and assay of SleB function

To create the $sleB^{E151A}$ allele in which the catalytic glutamate is changed to an alanine, PCR-based site-directed mutagenesis was carried out using the following primers: 5'CTCATGGCAAACGCAGTATACGGAGCGTCTCGTGGTG3' and 5'CACCACGAGACGCTCCGTATACTGCGTTTGCCATGAG3'. The alteration was made to the *sleB* gene in plasmid pDPV346 [6]. The resulting plasmid pDPV430 was introduced into strain DPBa74 [21] in order to test if the altered protein allows completion of spore germination. Spores were plated in the presence and absence of lysozyme as previously described[21].

Results

Structure solution and overall fold of $SleB_{CAT}$

Following an unsuccessful attempt to crystallize the full-length SleB, we focused on the structure of the catalytic domain encompassing residues 125 to 253 of the enzyme. We were unable to solve the structure by molecular replacement and therefore a MAD phasing strategy was employed. Ultimately, data collected from crystals of the selenomethionine-substituted $SleB_{CAT}^{L143M}$ variant permitted modeling of the two virtually identical molecules in the asymmetric unit. Cartoon and solvent accessible surface representations of one molecule are provided in Fig. 1a. The completed models made it immediately obvious why molecular replacement had not been successful: While there is a good structural correspondence between $SleB_{CAT}$ and the structures of other transglycosylases for a core region encompassing helices H1, H2, and H5, the overall structure of $SleB_{CAT}$ is distinct, particularly with respect to the topology of the active site. H1 contains the conserved catalytic residue, which is positioned at one end of the active site cleft by the other two core helices. In addition, the large H2 helix also forms the floor of this cleft. Beyond this minimal structural conservation a search of the protein data bank (PDB) for related structures produced only a single protein with more extensive structural homology to $SleB_{CAT}$ belonging to the *E. coli* lytic PG transglycosylase YceG (pdb code 2R1F). The root-mean-square-deviation for the backbones of the forty-seven overlapping amino acids was 2.5Å (Fig. 2a). $SleB_{CAT}$ has an approximately globular shape, measuring ~46Å, 36Å, and 30Å along its three longest perpendicular axes. While primarily an alpha helical protein, a large portion of the active site is formed by a three-stranded antiparallel beta sheet, also preserved in YceG. The 15Å-deep active site cleft measures about 27Å end-to-end; its width varying between 10Å and 13Å over the length of the cleft.

Identification of the catalytic glutamate residue of SleB and CwlJ

The active site clefts of PG transglycosylases contain five or more subsites for binding ring-shaped carbohydrate moieties. For instance, the bacteriophage φKZ enzyme gp144 contains five subsites -4 to +1 and cleavage occurs between the NAM and NAG moieties bound in sites -1 and +1 [22]. The mechanism whereby lytic transglycosylases catalyze the generation of the characteristic 1,6-anhydromuramic acid product is not fully understood. According to the currently held model, the cleavage reaction requires a single glutamate and the N-acetyl group of the NAM moiety bound to the -1 subsite [22,23]. Cleavage is initiated by the N-acetyl oxygen, which carries out a nucleophilic attack on the C1-atom of the NAM group. The glutamate is believed to stabilize the first transition state of the reaction by donating a proton to the forming hydroxyl group of the departing NAG moiety. The glutamate is also thought to stabilize the second transition state when the C6-hydroxyl of the terminal NAM moiety displaces the N-acetyl oxygen at the C1 position to give the final product (Supplementary Figure S1).

The low degree of sequence similarity between SleB and other lytic transglycosylases where the catalytic glutamate had already been identified prevented the determination of the catalytic residue of SleB until now. However, the functionally similar enzymes display a higher degree of conservation at the tertiary structure level. Therefore a least-square superposition of the $SleB_{CAT}$ structure with Slt-70 [24], bacteriophage φKZ lytic transglycosylase gp144 [22] and the to-date unpublished but pdb-deposited structure of a lytic transglycosylase YceG from *E .coli* precisely overlaid residue E151 of SleB with glutamates in the other enzymes. In all cases this residue is strictly conserved and positioned near one end of the large substrate-binding cleft at the very end of a large helix. The essential role of this positionally conserved glutamate in catalysis has been confirmed for both gp144 and Slt-70 [22,24]. A second glutamate, E-155 in $SleB_{CAT}$, is also conserved among SleB-type

enzymes and is positioned in a loop region that marks the edge of the binding cleft, suggesting that this residue might form part of the +1 site required for NAG binding.

We created a version of *sleB* in which the catalytic E-151 was changed to an alanine and tested for SleB function in allowing completion of germination. Spores lacking *cwlJ1* and *sleB* are unable to complete germination and form colonies[6] (Supplementary Table S2). Complementation with a plasmid bearing *sleB* restores function, but the same plasmid bearing $sleB^{E151A}$ did not. The ability of a limited application of external lysozyme to rescue these spores' colony-forming ability indicates that their germination defect is in cortex degradation.

In addition to SleB, *B. anthracis* produces a second GSLE specific for the cleavage of cortex PG, CwlJ1 [6]. Functionally redundant with SleB, this enzyme possesses no PG-binding domain but its catalytic domain displays 40% sequence identity with SleB. CwlJ1 features a close succession of three glutamate residues in the region that likely contains the catalytic amino acid, making its identification complicated. However, the close similarity of CwlJ1 and SleB sequences allowed the construction of a homology model of CwlJ1, which in turn enabled us to predict that E21 mediates catalysis in this enzyme, while E23 and E25 are likely involved in NAG binding in the +1 site.

Conserved and unique features of the peptidoglycan binding cleft of $SleB_{CAT}$

$SleB_{CAT}$ displays a number of unique structural features beyond the conserved positions of a core of three helices. The structure most similar to $SleB_{CAT}$ is that of the YceG enzyme from *E. coli*. Therefore, we focused our analysis of the carbohydrate-binding cleft on a comparison of these two proteins. Because *E. coli* does not produce muramic-δ-lactam-containing PG, this comparison was particularly helpful with discerning between universally conserved features of the $SleB_{CAT}$ active site and features that are potentially reflective of the unique substrate specificity of SleB. Characteristic of carbohydrate-binding sites, the binding clefts of both enzymes are lined with a number of aromatic amino acids. Fig. 2a depicts the superposition of $SleB_{CAT}$ and *E. coli* YceG. Shown in Fig. 2c are the side chains of residues that are structurally conserved. $SleB_{CAT}$ residue F190 and F232 of the *E. coli* enzyme are also included because their side chains occupy a very similar space in the pocket even though they are not related at the primary structure level. Similarities in the folds of the two proteins and in the topologies of the binding clefts are particularly pronounced near the catalytic residues. This is consistent with the fact that the substrates of the two enzymes do not differ in the regions that bind to subsites -2, -1, and +1. A fascinating aspect about GSLEs is the question of how these enzymes achieve specificity for the muramic-δ-lactam moiety that binds in the -3 site. Fig. 2d is an extension of Fig. 2c to now include the side chains of residues that are present in $SleB_{CAT}$ but not in the *E. coli* enzyme. Intriguingly, these residues are clustered around a relatively small part of the binding pocket. In order to determine if this region of SleB is responsible for muramic-δ-lactam recognition we attempted to co-crystallize $SleB_{CAT}$ with a tetrasaccharide muropeptide containing muramic-δ-lactam (Muropeptide Q, Tetrasaccharide-Ala in reference [6]), which was similar to an SleB product. Because this was unsuccessful, we examined the ligand-binding modes in the complexes of the related bacteriophage gp144 enzyme with chitotetraose and of *E. coli* transglycosylase SLT70 in complex with the inhibitor Bulgecin A. In both cases the ligands are bound in an extended orientation (Fig. 2b). Especially, the relative positions of the two rings bound to the -2 and -1 sites are very similar. In this extended conformation the ring of the chitotetraose that is bound to the -3 site of gp144 is positioned about 11Å away from the carboxylate group of the catalytic glutamate. If we assume that SleB binds substrate to subsites -2 and -1 as observed in the other two enzymes, then the approximate position of the unique -3 site can be inferred. This approach suggests that SleB residues F176, P187, R188, W236, and perhaps even S234 form the -3 subsite, i.e. all residues

located in structurally unique regions of SleB. Consistent with the hypothesis that F176, P187, and W236 play a role in the binding of muramic-δ-lactam, the three residues are not only conserved among SleB homologues but also in CwlJ where F48, P62, and W114 occupy the corresponding positions in the sequence (Supplementary file S3). It should be noted that there is a group of closely related SleB-type proteins, typified by *B. subtilis* YkvT, which should not specifically function in the degradation of cortex PG [12], but the above listed residues are conserved here as well. Therefore, it is possible that these residues are necessary but not sufficient for the exclusive specificity of SleB for muramic-δ-lactam. In addition, the specificity might be fine-tuned by the next tier of amino acids that acts as scaffolding for the active site and ensures proper positioning of backbone and side chain atoms.

The entrance of the $SleB_{CAT}$ substrate binding cleft is shaped by a metal binding site

A surprising feature of the $SleB_{CAT}$ structure was the discovery of a bound metal ion near the putative -4 subsite of the binding cleft. The metal ion is octahedrally coordinated by five backbone carbonyl groups of residues from a loop region that bridges helices H2 and H3 and the side chain oxygen of asparagine N178. The six ligand atoms are all positioned about 2.4 Å away from the ion. This distance is characteristic for complexes of either Ca^{+2} and Na^{+1} ions, while Mg^{2+} was dismissed based on the observation that it forms shorter bonds of around 2.1Å [25]. The addition of the calcium-chelating agent EGTA to a previously described *in vitro* assay [15] had no significant impact on SleB activity. Moreover, modeling a calcium ion into the $SleB_{CAT}$ structure produced negative density in the F_o-F_c map, which indicates that either the site is only partially occupied or that the actual ion has fewer electrons. Lastly, when EGTA was included during crystallization this had no impact on the height of the electron density peak leading us to conclude that calcium was not bound to this site. Therefore, even though a metal analysis showed slightly elevated calcium levels in the protein sample compared to the reference buffer, we concluded that the observed ion is most likely a Na^{+1}. The conspicuous position of the metal binding site at the entrance of the substrate binding pocket is intriguing, however, the biological role of the metal ion remains to be explored.

Discussion

The presented crystal structure of the SleB catalytic domain places this enzyme within the Slt family of (PF01464) lytic transglycosylases. While other lytic enzymes have been shown to be promiscuous, cleaving both cortex and conventional PG, SleB requires the presence of the muramic-δ-lactam structure for its activity and does not act on regular PG. Therefore, testing our predictions concerning the muramic-δ-lactam-binding pocket may not be easy because mutations in this region could not only cause a loss of specificity for muramic-δ-lactam but also produce an enzyme that is inactive on all substrates. Additional structural studies of SleB-substrate complexes might be able to clarify this unique substrate specificity.

Supplementary Material

Refer to Web version on PubMed Central for supplementary material.

Acknowledgments

Funding in part was provided by Public Health Service grant AI060726 from the National Institute of Allergy and Infectious Diseases. Funding for data collected at beamline 29 NSLS is provided by DOE/DER and NIH/NCRR.

Abbreviations

Cwlj	Cell wall hydrolase j
DTT	Dithiothreitol
EGTA	ethylene glycol tetraacetic acid
GSLEs	germination specific lytic enzymes
MAD	multiple-wavelengths anomalous dispersion
MBP	maltose binding protein
NAG	N-acetylglucosamine
NAM	N-acetylmuramic acid
Ni-NTA	nickel-nitriloacetic acid
PG	peptidoglycan
SleB	spore cortex lytic enzyme B
$SleB_{CAT}$	catalytic domain of SleB

REFERENCES

1. Setlow P. Spores of *Bacillus subtilis*: their resistance to and killing by radiation, heat and chemicals. J Appl Microbiol. 2006; 101(3):514–525. [PubMed: 16907802]
2. Popham DL, Helin J, Costello CE, Setlow P. Muramic lactam in peptidoglycan of *Bacillus subtilis* spores is required for spore outgrowth but not for spore dehydration or heat resistance. Proc Natl Acad Sci U S A. 1996; 93(26):15405–15410. [PubMed: 8986824]
3. Setlow B, Melly E, Setlow P. Properties of spores of *Bacillus subtilis* blocked at an intermediate stage in spore germination. J Bacteriol. 2001; 183(16):4894–4899. [PubMed: 11466293]
4. Koshikawa T, Beaman TC, Pankratz HS, Nakashio S, Corner TR, Gerhardt P. Resistance, germination, and permeability correlates of *Bacillus megaterium* spores successively divested of integument layers. J Bacteriol. 1984; 159(2):624–632. [PubMed: 6430874]
5. Boland FM, Atrih A, Chirakkal H, Foster SJ, Moir A. Complete spore-cortex hydrolysis during germination of *Bacillus subtilis* 168 requires SleB and YpeB. Microbiology. 2000; 146:57–64. [PubMed: 10658652]
6. Heffron JD, Orsburn B, Popham DL. Roles of germination-specific lytic enzymes CwlJ and SleB in *Bacillus anthracis*. Journal of Bacteriology. 2009; 191(7):2237–2247. [PubMed: 19181808]
7. Moriyama R, Hattori A, Miyata S, Kudoh S, Makino S. A gene (*sleB*) encoding a spore cortex-lytic enzyme from *Bacillus subtilis* and response of the enzyme to L-alanine-mediated germination. Journal of Bacteriology. 1996; 178(20):6059–6063. [PubMed: 8830707]
8. Popham, DL.; Heffron, JD.; Lambert, EA. Degradation of Spore Peptidoglycan During Germination.. In: Abel-Santos, E., editor. Bacterial Spores: Current Research and Applications. Caister Academic Press; Norwich, UK: 2012.
9. Moriyama R, Fukuoka H, Miyata S, Kudoh S, Hattori A, Kozuka S, Yasuda Y, Tochikubo K, Makino S. Expression of a germination-specific amidase, SleB, of Bacilli in the forespore compartment of sporulating cells and its localization on the exterior side of the cortex in dormant spores. Journal of Bacteriology. 1999; 181(8):2373–2378. [PubMed: 10197998]
10. Moriyama R, Kudoh S, Miyata S, Nonobe S, Hattori A, Makino S. A germination-specific spore cortex-lytic enzyme from *Bacillus cereus* spores: cloning and sequencing of the gene and molecular characterization of the enzyme. Journal of Bacteriology. 1996; 178(17):5330–5332. [PubMed: 8752358]
11. Chen Y, Fukuoka S, Makino S. A novel spore peptidoglycan hydrolase of *Bacillus cereus*: biochemical characterization and nucleotide sequence of the corresponding gene, *sleL*. Journal of Bacteriology. 2000; 182(6):1499–1506. [PubMed: 10692353]

12. Chirakkal H, O'Rourke M, Atrih A, Foster SJ, Moir A. Analysis of spore cortex lytic enzymes and related proteins in *Bacillus subtilis* endospore germination. Microbiology. 2002; 148(8):2383–2392. [PubMed: 12177332]

13. Warth AD, Strominger JL. Structure of the peptidoglycan of bacterial spores: occurrence of the lactam of muramic acid. Proc Natl Acad Sci USA. 1969; 64:528–535. [PubMed: 4982357]

14. Ishikawa S, Yamane K, Sekiguchi J. Regulation and characterization of a newly deduced cell wall hydrolase gene (*cwlJ*) which affects germination of *Bacillus subtilis* spores. Journal of Bacteriology. 1998; 180(6):1375–1380. [PubMed: 9515903]

15. Heffron JD, Sherry N, Popham DL. In vitro studies of peptidoglycan binding and hydrolysis by the *Bacillus anthracis* germination-specific lytic enzyme SleB. Journal of Bacteriology. 2011; 193(1): 125–131. [PubMed: 20971910]

16. Laboratory SD. COLLABORATIVE COMPUTATIONAL PROJECT, NUMBER 4. 1994. “The CCP4 Suite: Programs for Protein Crystallography”. Acta Cryst D. 1994; 50:760–763. [PubMed: 15299374]

17. Hendrickson WA, Horton JR, LeMaster DM. Selenomethionyl proteins produced for analysis by multiwavelength anomalous diffraction (MAD): a vehicle for direct determination of three-dimensional structure. EMBO J. 1990; 9(5):1665–1672. [PubMed: 2184035]

18. Adams PD, Afonine PV, Bunkoczi G, Chen VB, Davis IW, Echols N, Headd JJ, Hung LW, Kapral GJ, Grosse-Kunstleve RW, McCoy AJ, Moriarty NW, Oeffner R, Read RJ, Richardson DC, Richardson JS, Terwilliger TC, Zwart PH. PHENIX: a comprehensive Python-based system for macromolecular structure solution. Acta Crystallogr D Biol Crystallogr. 2010; 66(Pt 2):213–221. [PubMed: 20124702]

19. Emsley P, Lohkamp B, Scott WG, Cowtan K. Features and development of Coot. Acta Crystallogr D Biol Crystallogr. 2010; 66(Pt 4):486–501. [PubMed: 20383002]

20. Laskowski RA, Macarthur MW, Moss DS, Thornton JM. Procheck - a Program to Check the Stereochemical Quality of Protein Structures. J Appl Crystallogr. 1993; 26:283–291.

21. Heffron JD, Lambert EA, Sherry N, Popham DL. Contributions of four cortex lytic enzymes to germination of *Bacillus anthracis* spores. J Bacteriol. 2010; 192(3):763–770. [PubMed: 19966006]

22. Fokine A, Miroshnikov KA, Shneider MM, Mesyanzhinov VV, Rossmann MG. Structure of the bacteriophage phi KZ lytic transglycosylase gp144. J Biol Chem. 2008; 283(11):7242–7250. [PubMed: 18160394]

23. Scheurwater E, Reid CW, Clarke AJ. Lytic transglycosylases: bacterial space-making autolysins. Int J Biochem Cell Biol. 2008; 40(4):586–591. [PubMed: 17468031]

24. Thunnissen AM, Rozeboom HJ, Kalk KH, Dijkstra BW. Structure of the 70-kDa soluble lytic transglycosylase complexed with bulgecin A. Implications for the enzymatic mechanism. Biochemistry. 1995; 34(39):12729–12737. [PubMed: 7548026]

25. Harding MM. Small revisions to predicted distances around metal sites in proteins. Acta Crystallogr D Biol Crystallogr. 2006; 62(Pt 6):678–682. [PubMed: 16699196]

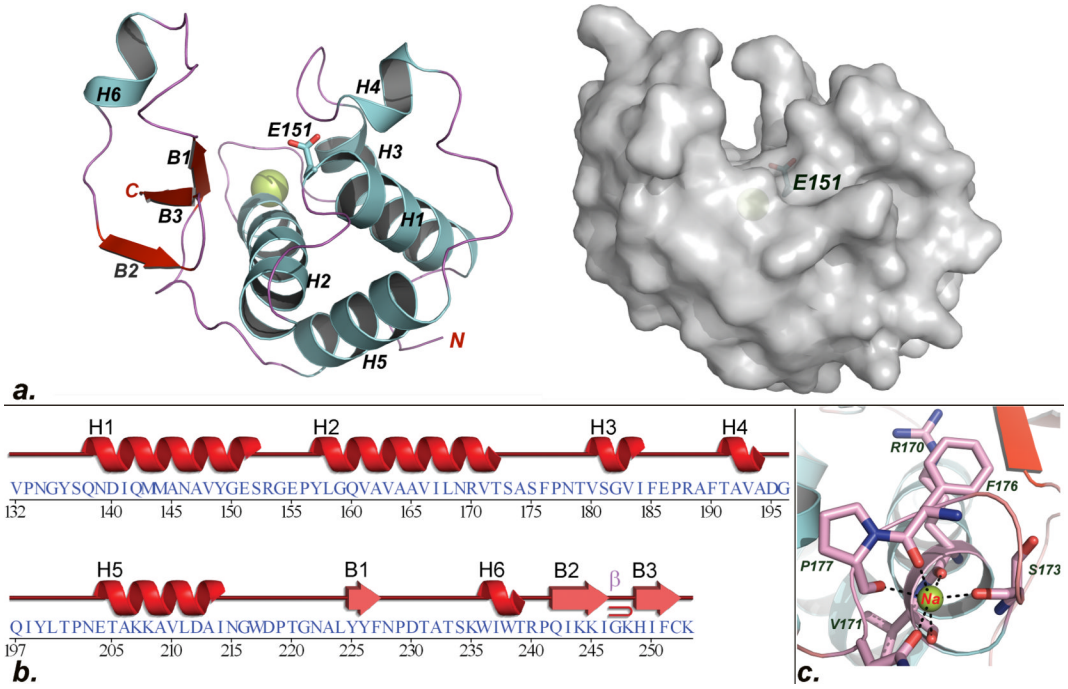

Fig.1. Crystal structure of SleB$_{CAT}$

a. Cartoon and surface depictions of the SleB$_{CAT}$ structure. The sodium ion is shown as a yellow sphere and the side chain of the catalytic glutamate is depicted in the stick format. **b.** Summary of correlation between SleB$_{CAT}$ sequence and secondary structure topology. **c.** Schematic presentation of the metal binding site formed by residues from a loop region encompassing amino acids 170 to 178.

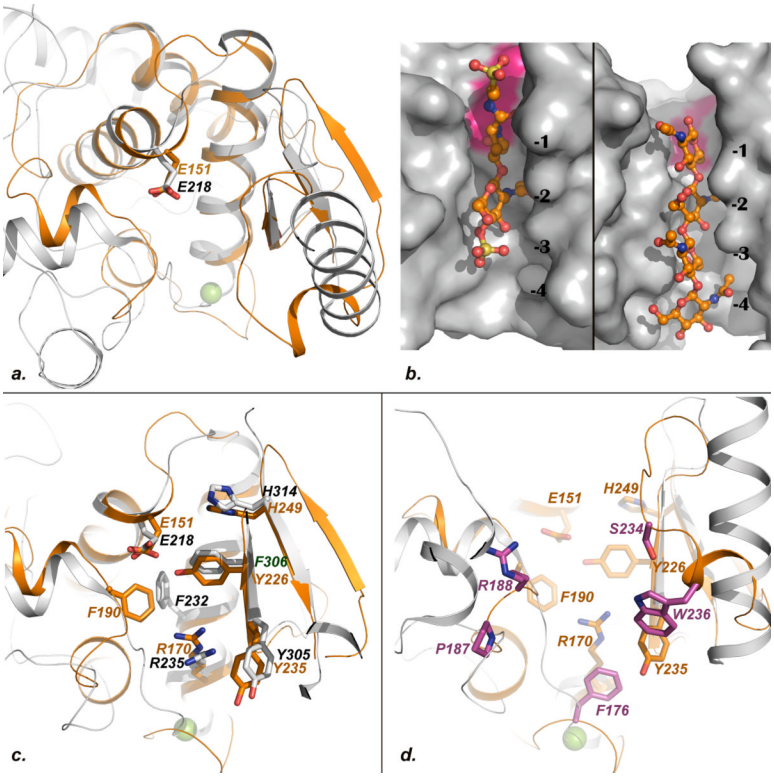

Fig.2. Mapping of conserved and unique features of the SleB$_{CAT}$ active site

a. Superposition of SleB (orange) and YceG (gray, pdb code 2R1F). b. Close-up view of the Slt-70-bulgecin (left) and gp144-chitotetraose (right) complexes showing the extended binding modes of the ligands. **c**. Superposition of SleB (orange) and YceG (gray) backbones showing the side chains of structurally conserved residues from both protein. **d.** Superposition of SleB (orange) and YceG (gray) showing the side chains of SleB residues that are structurally conserved with YceG in orange and those that are unique to SleB in magenta.

Table I

Data Collection and Refinement Statistics for the SeMet-SleB$_{CAT}^{L143M}$ Crystal Structure

(A) Data collection statistics			
Space group	$P22_12_1$		
molecules/asymmetric unit	2		
Cell parameters (Å)	a = 53.9, b = 64.5, c = 84.0		
Wavelength (Å)	0.9792	0.9611	0.9794
Resolution (Å)	30.34 - 1.9 (1.9-2.0)	30 - 1.9 (1.9-2.0)	30 - 2.0 (2.0-2.11)
Completeness (%) (last shell)[a]	99.3 (100)	99.2 (98.3)	99.1 (98.6)
Redundancy	12.8 (13.9)	12.5 (12.1)	11.9 (11.5)
I/σ	19.4 (5.0)	23.3 (4.6)	22.5 (4.6)
R_{merge} (%)[b]	9.1 (51.5)	6.8 (55.3)	7.2 (54.1)
No. of unique reflections	23743	23899	23892
No. of measured reflections	849540	1025839	1079414
(B) Refinement statistics			
Resolution range (Å)	33.22 - 1.91		
R (%)[c]/ R_{free} (%)[d]	20.51/24.87		
rms bonds (Å)/ rms angles (°)	0.02/2		
Number of protein atoms	1896		
Number of water atoms	319		
Overall mean B factor value (Å^2)	13.95		
Wilson plot B value	13.45		
Ramachandran analysis (%)			
Most favored	95		
Allowed	5		
Disallowed	0		

[a] Values in parentheses relate to the highest resolution shell.

[b] $R_{\text{merge}} = \Sigma|I - \langle I \rangle| / \Sigma I$, where I is the observed intensity, and $\langle I \rangle$ is the average intensity obtained from multiple observations of symmetry-related reflections after rejections.

[c] $R = \Sigma||F_O| - |F_C||/\Sigma|F_O|$, where F_O and F_C are the observed and calculated structure factors, respectively.

[d] R_{free} defined in Brunger[25].